Electronic Supplementary Material (ESI) for Journal of Materials Chemistry A.

Supporting Information

Spatially Separated Catalytic Sites Supplied with CdS-MoS_2-In_2O_3 Ternary Dumbbell S-scheme heterojunction For Enhanced Photocatalytic Hydrogen Production

Lijun Zhang[1,2], Xudong Jiang[1], Zhiliang Jin [1]*, Noritatsu Tsubaki [2]*

1. School of Chemistry and Chemical Engineering, North Minzu University, Yinchuan 750021, P.R.China

2. Department of Applied Chemistry, Graduate School of Engineering, University of Toyama, Gofuku 3190, Toyama 930-8555, Japan

Corresponding author: zl-jin@nun.edu.cn, (Z. Jin) tsubaki@eng.u-toyama.ac.jp (N. Tsubaki).

1. Experimental details Supplement

1.1 Characterization methods

The morphology and crystal structure of the photocatalyst is understood by Zeiss evo10 scanning electron microscope, FEI tecnai G2 transmission electron microscope, and HORIBA Scientific X-ray diffractometer. The valence state analysis of the surface elements of the photocatalyst was performed on the ESCALAB Xi+ X-ray Photoelectron Spectrometer instrument. In-situ irradiated XPS measurements of samples with external light source irradiation (λ = 310 nm, Shenzhen Lamplic Technology Co., Ltd.) UV-Vis-NIR diffuse reflectance spectroscopy (UV-Vis-NIR DRS) was measured using Shimadzu UV-2550 spectrometer, with $BaSO_4$ as the background. ASAP2460M was used to obtain the nitrogen adsorption-desorption isotherm of the sample at 77 K. Electron paramagnetic resonance (EPR) testing of hydroxyl and superoxide radicals was performed using a German Bruker A300-10/12. Use FLUOROMAX-4 spectrophotometer for photoluminescence spectrum test. The photoelectrochemical test was carried out in 0.2 M $NaSO_4$ solution using VersaStat4-400 electrochemical workstation.

1.2 Hydrogen production experiments

The PCX-50B multi-channel photochemical reaction system of Beijing Perfectlight is used to test the performance of photocatalytic hydrogen production. A quartz bottle with a flat window at the bottom was used as the reaction vessel. The simulated solar light source is a white light 5 W LED lamp and 300 W Xe lamp (with 420 nm cut-off filter, $\lambda \geq 420$ nm), and 10 mg photocatalyst is dispersed in 10 vol% lactic acid aqueous solution. After using ultrasonic dispersion, the system air is replaced by nitrogen. Finally, a Tianmei GC7900 gas chromatograph was used to detect hydrogen. The chromatographic column is 13X, the carrier gas is N_2, and it is equipped with a TCD detector. The H_2 output is determined by the external standard method. The containers and experimental procedures used in the hydrogen production experiment under the natural sun are the same as those operated under the simulated solar light source. The apparent quantum efficiency (AQE) is calculated according to the following formula:

$$AQE = \frac{number\ of\ reacted\ electrons}{number\ of\ incident\ photons} \times 100\%$$

$$= \frac{2 \times number\ of\ evolved\ H_2\ molecules}{number\ of\ incident\ photons} \times 100\%$$

2. Supporting Figures and Table

Figure.S1. XRD patterns of the (a) MoS_2; (b) In_2O_3; (c) CdS-Mx (x=1, 2, 3, 4.) and (d) CdS-Inx (x= 10%, 20%, 30%, 40%, 50%.) samples.

Figure.S2. (d, e) N_2 adsorption-desorption isotherms of CdS, MoS_2, In_2O_3, CdS-M2, CdS-In30% and CdS-M2-In30%.

Figure.S3. The pore size distribution curves of CdS, CdS-M2, CdS-In30% and CdS-M2-In30%.

Figure.S4. SEM morphologies of the MoS_2 (a); Element mapping test of CdS-M2 (b); In-MOFs (c); In_2O_3 (d).

Figure.S5. XRD comparison of CdS-M2-In30% photocatalyst before and after illumination.

Figure.S6. SEM comparison of the CdS-M2-In30% photocatalyst before and after the reaction.

Figure.S7. Comparison of fine spectra of S 2p XPS before and after the CdS-M2-In30% photocatalyst reaction.

Figure.S8. Photocatalyst coated electrode schematic.

Figure.S9. UV-Vis-NIR diffuse reflectance curves of MoS_2 (a) and In_2O_3 (b). Kubelka-Munk function and energy graph of In_2O_3 (c) and CdS (d).

Figure.S10. The schematic diagram of the scattering/reflection effect for the incident light on the surface of a Hollow structure.

Figure.S11. CdS(a) and In_2O_3 (b) Mott-Schottky curve.

Figure.S12. CdS and In_2O_3 Schematic diagram of the energy band.

Figure.S13. Schematic diagram of photo-generated electron flow between semiconductors before and after CdS-In_2O_3 catalyst is illuminated.

Table S1. Parameters of CdS, MoS_2, In_2O_3, CdS-M_2(CdS-MoS_2), CdS-In30%(CdS-In_2O_3), and CdS-M2-In30%(CdS-MoS_2-In_2O_3) were obtained from the analysis of N_2.

Table S2. Attenuation parameters of the catalyst.

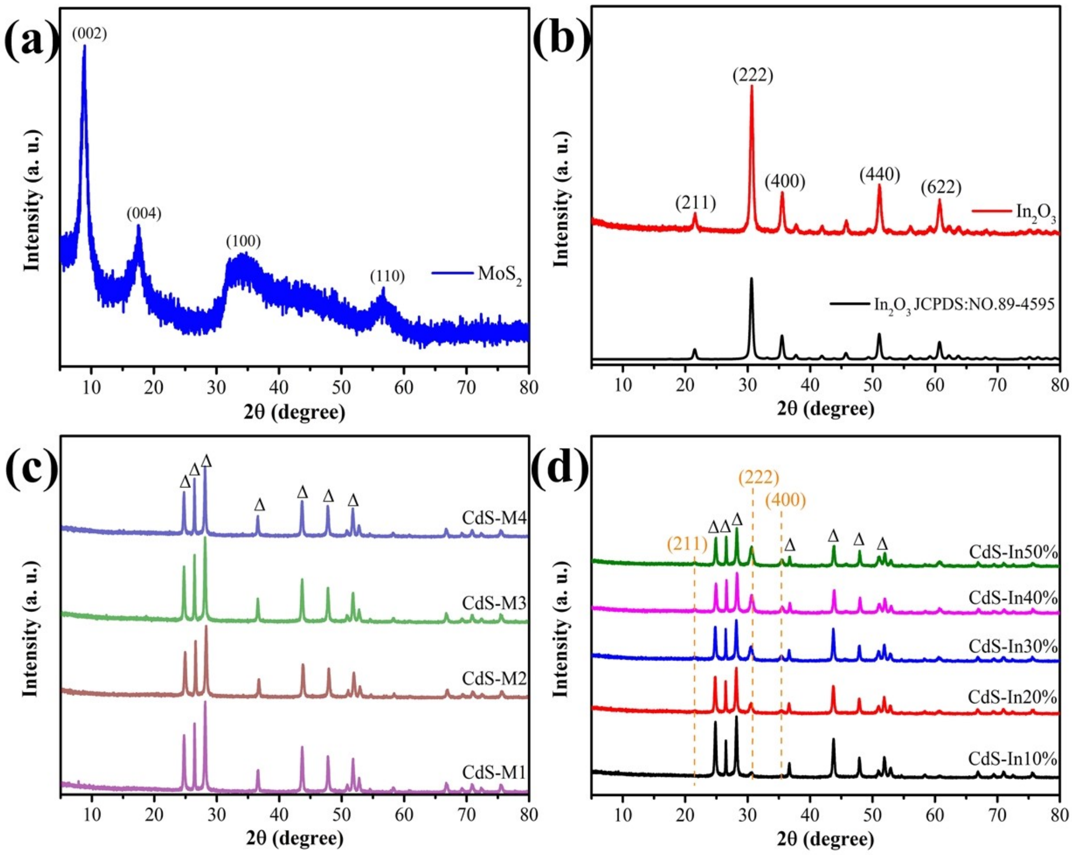

Figure.S1. XRD patterns of the (a) MoS_2; (b) In_2O_3; (c) CdS-Mx (x=1, 2, 3, 4.) and (d) CdS-Inx (x= 10%, 20%, 30%, 40%, 50%.) samples.

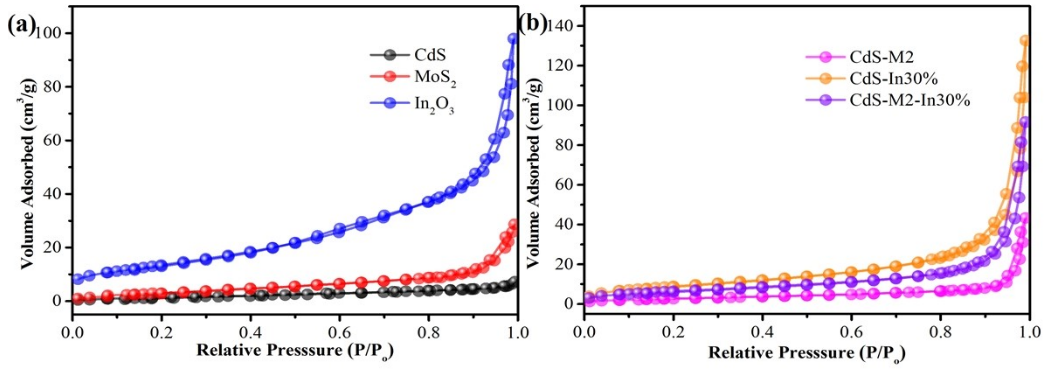

Figure.S2. (a, b) N_2 adsorption-desorption isotherms of CdS, MoS_2, In_2O_3, CdS-M2(CdS-MoS_2), CdS-In30%(CdS-In_2O_3) and CdS-M2-In30%(CdS-In_2O_3-MoS_2).

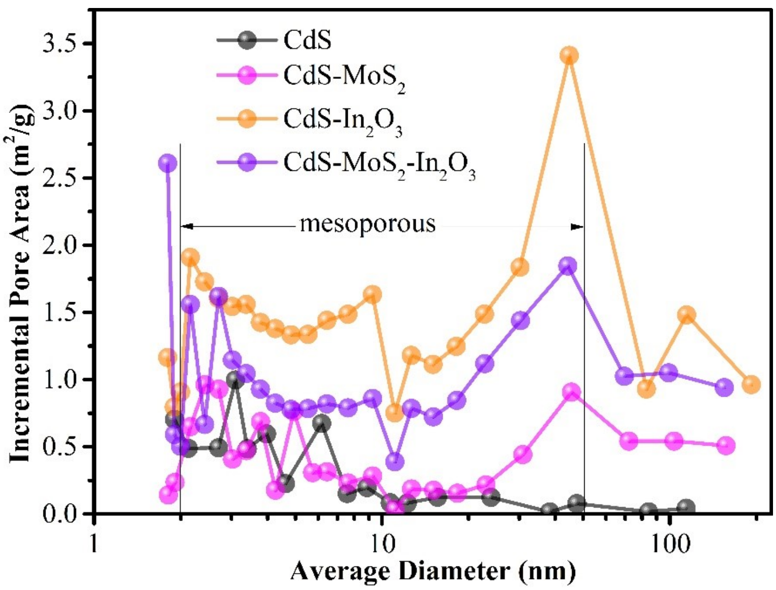

Figure.S3. The pore size distribution curves of CdS, CdS-M2, CdS-In30% and CdS-M2-In30%.

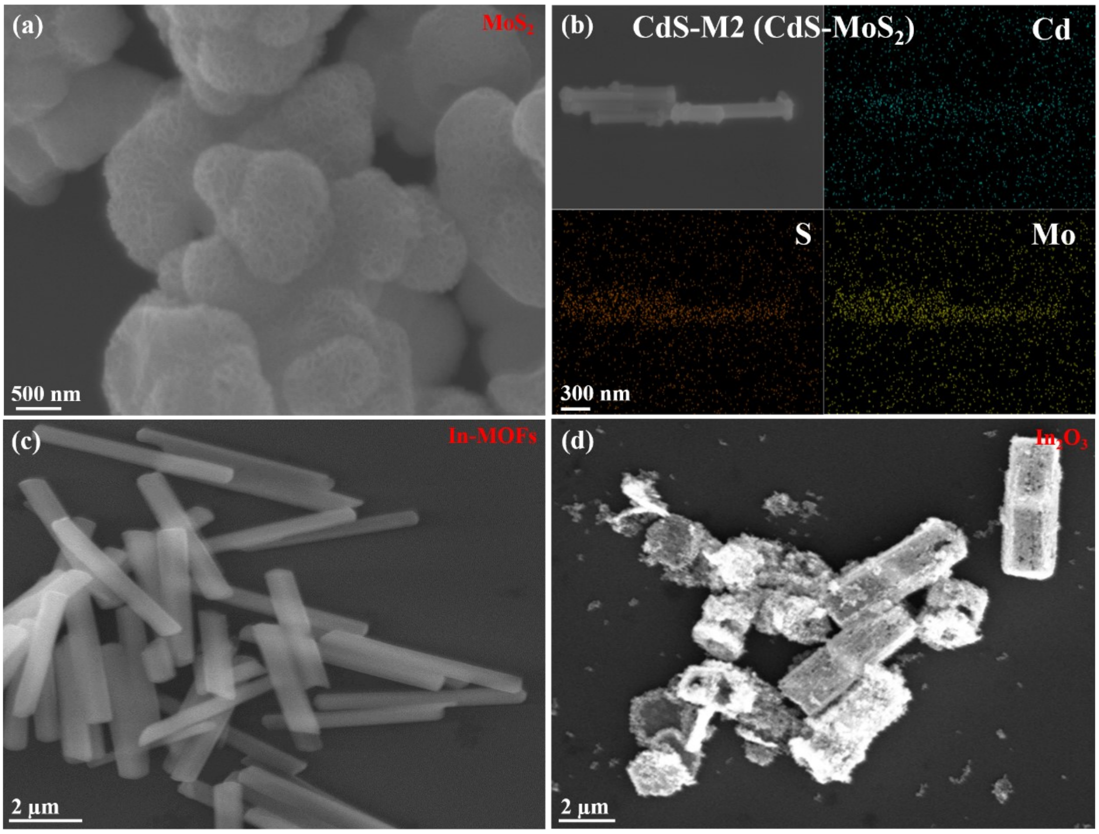

Figure.S4. SEM morphologies of the MoS_2 (a); Element mapping test of CdS-M2 (b); In-MOFs (c); In_2O_3 (d).

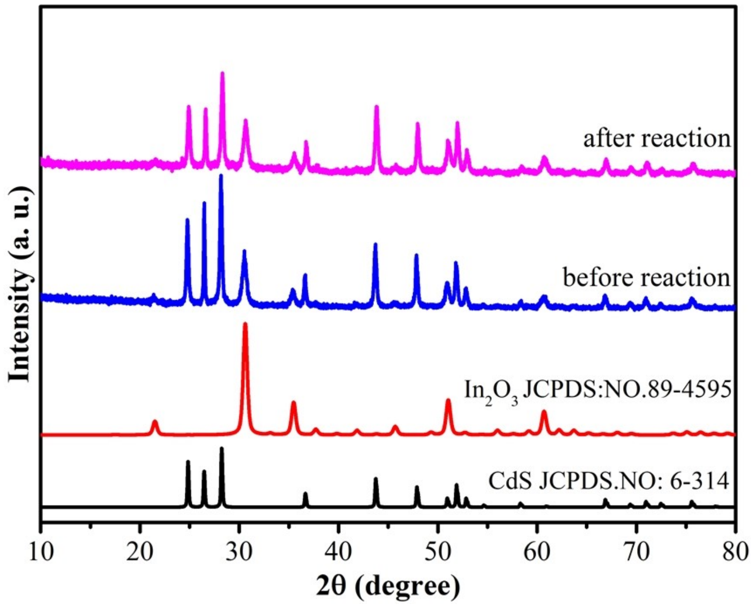

Figure.S5. XRD comparison of CdS-M2-In30% photocatalyst before and after illumination.

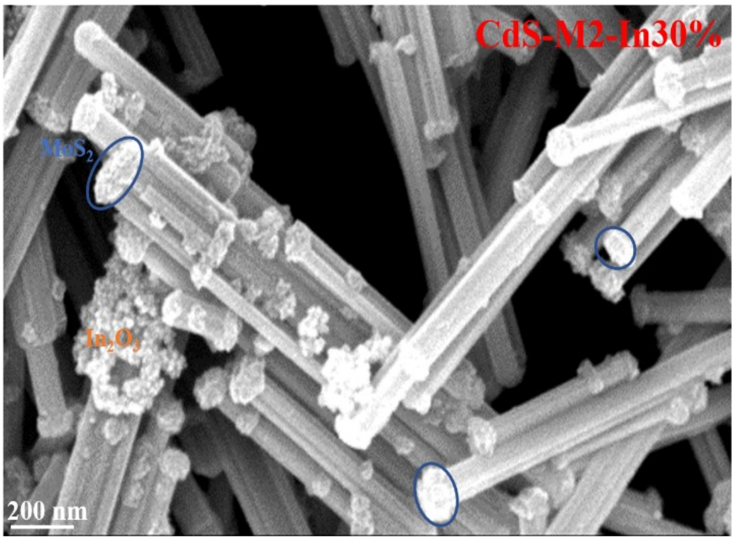

Figure.S6. SEM comparison of the CdS-M2-In30% photocatalyst before and after the reaction.

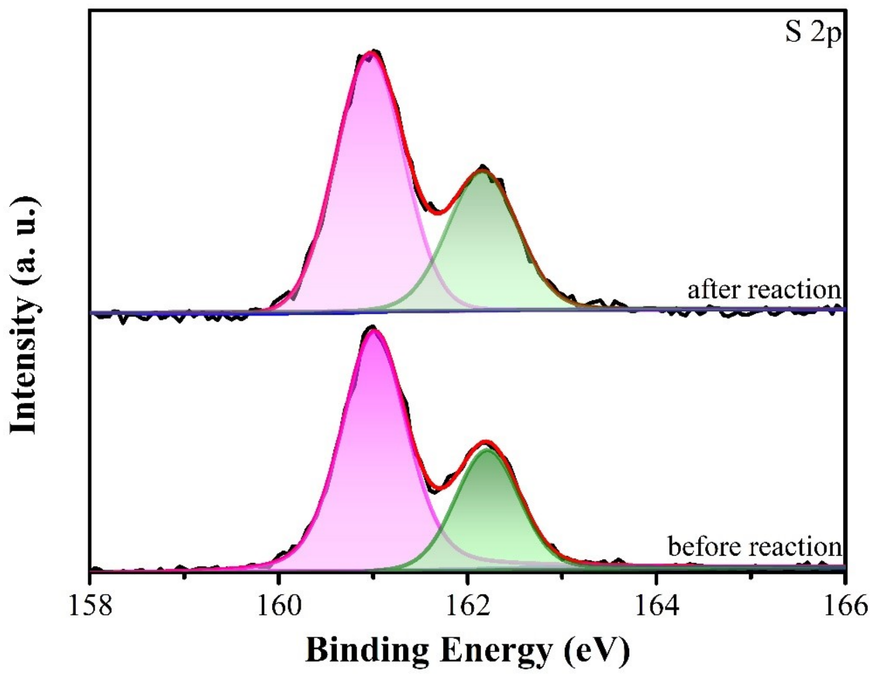

Figure.S7. Comparison of fine spectra of S 2p XPS before and after the CdS-M2-In30% photocatalyst reaction.

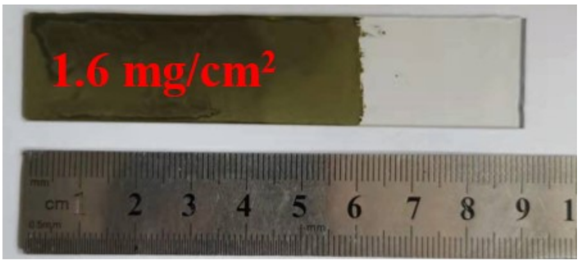

Area: 2cm × 6cm

Figure. S8. Photocatalyst coated electrode schematic.

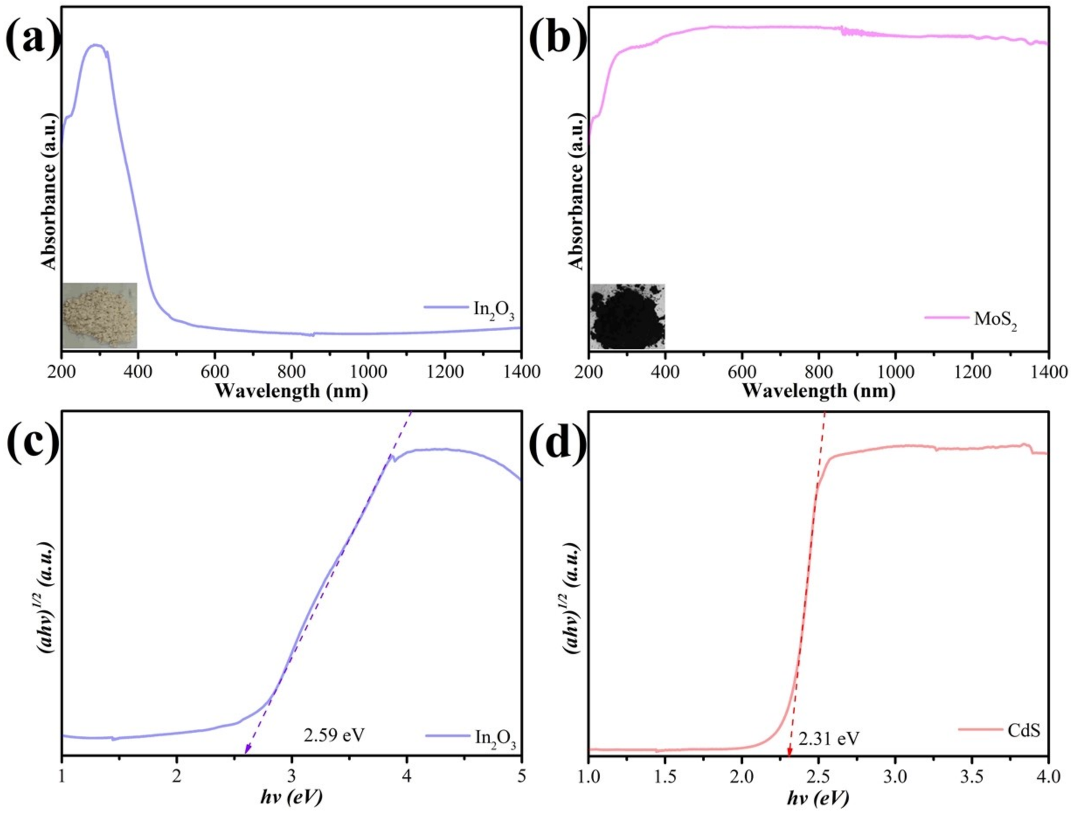

Figure.S9. UV-Vis-NIR diffuse reflectance curves of MoS_2 (a) and In_2O_3 (b). Kubelka-Munk function and energy graph of In_2O_3 (c) and CdS (d).

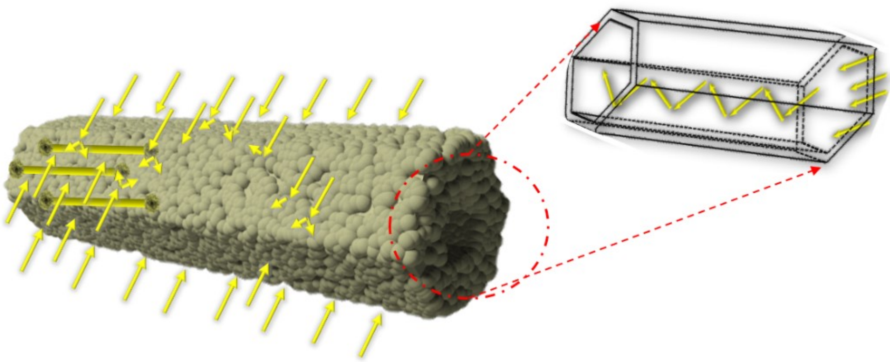

Figure.S10. The schematic diagram of the scattering/reflection effect for the incident light on the surface of a Hollow structure.

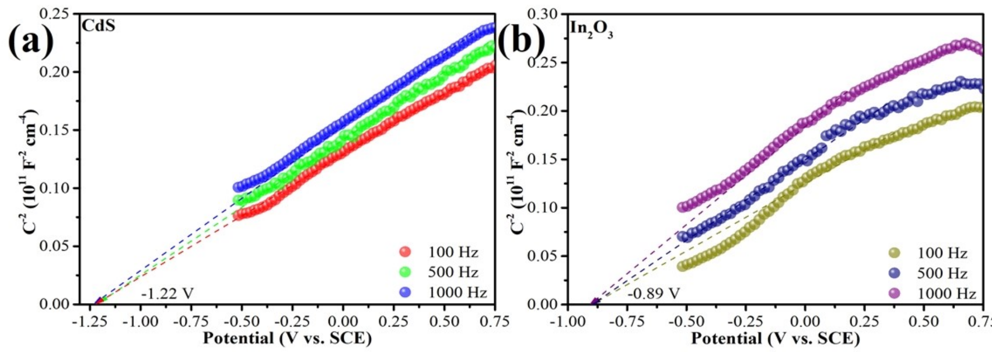

Figure.S11. CdS(a) and In_2O_3 (b) Mott-Schottky curve.

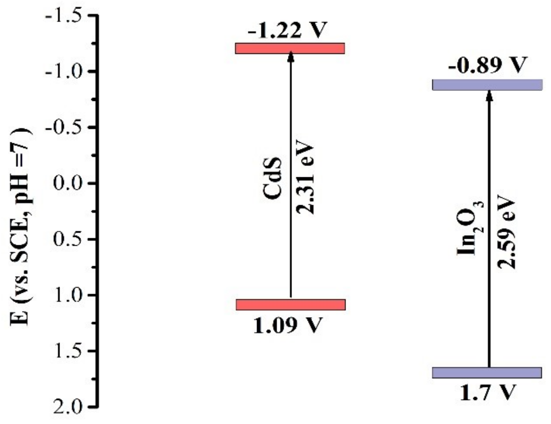

Figure.S12. CdS and In_2O_3 Schematic diagram of the energy band.

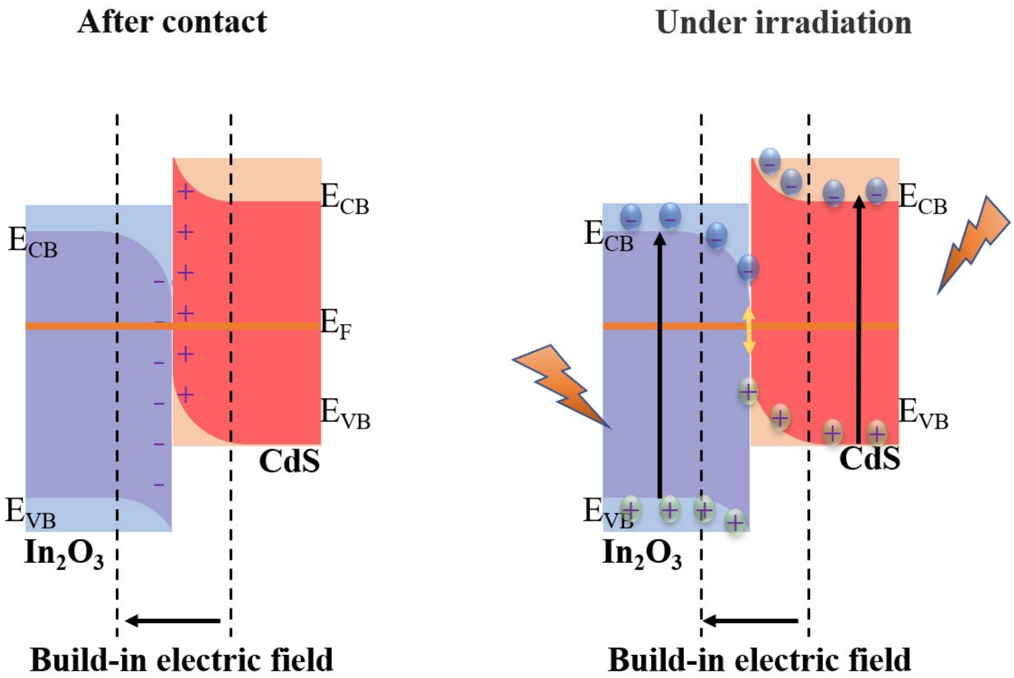

Figure.S13. Schematic diagram of photo-generated electron flow between semiconductors before and after CdS-In_2O_3 catalyst is illuminated.

Table S1. Parameters of CdS, MoS_2, In_2O_3, CdS-M_2(CdS-MoS_2), CdS-In30%(CdS-In_2O_3), and CdS-M2-In30%(CdS-MoS_2-In_2O_3) were obtained from the analysis of N_2.

Samples	S_{BET}	Pore volume	Average pore size
CdS	5 m^2g^{-1}	0.01 cm^3g^{-1}	7 nm
MoS_2	12 m^2g^{-1}	0.04 cm^3g^{-1}	13 nm
In_2O_3	49 m^2g^{-1}	0.15 cm^3g^{-1}	12 nm
CdS-MoS_2	9 m^2g^{-1}	0.06 cm^3g^{-1}	27 nm
CdS-In_2O_3	33 m^2g^{-1}	0.20 cm^3g^{-1}	24 nm
CdS-MoS_2-In_2O_3	23 m^2g^{-1}	0.13 cm^3g^{-1}	23 nm

Table S2. Attenuation parameters of the catalyst.

Samples	Pre-exponential factors A	Lifetime	Average lifetime	χ^2
	A_1 = 35.53	τ_1 = 5.071 ns		
CdS	A_2 = 21.62	τ_2 = 128.5 ns	1.952 ns	1.55
	A_3 = 42.85	τ_3 = 0.972 ns		
	A_1 = 34.39	τ_1 = 5.271 ns		
CdS-M2	A_2 = 23.00	τ_2 = 133.1 ns	2.116 ns	1.55
	A_3 = 42.61	τ_3 = 1.051 ns		
	A_1 = 42.66	τ_1 = 1.069 ns		
CdS-In30%	A_2 = 33.34	τ_2 = 5.322 ns	2.158 ns	1.57
	A_3 = 24.00	τ_3 = 140.1 ns		
	A_1 = 33.22	τ_1 = 5.310 ns		
CdS-M2-In30%	A_2 = 23.90	τ_2 = 138.6 ns	2.168 ns	1.56
	A_3 = 42.88	τ_3 = 1.080 ns		